A surface spectroscopic study of membranes fouled by pulp mill effluent
Carlsson, D. J.; Dal-Cin, Mauro; Black, P.; Lick, C. N.

National Research Council Canada   Conseil national de recherches Canada

Canada

A surface spectroscopic study of membranes fouled by pulp mill effluent[1]

D.J. Carlsson[*], M.M. Dal-Cin, P. Black, C.N. Lick

Institute for Chemical Process and Environmental Technology, National Research Council of Canada, Ottawa, Ontario, Canada K1A 0R6

Abstract

Infrared internal reflection spectroscopy (IR-IRS) and flux decline has been used to examine the build-up of adsorbed foulants on the surfaces of membranes during the treatment of the plug screw feed pressate (PSFP) from the sulfite digestion of wood chips. Of the four commercial membranes studied, hydrophillic cellulose and thin film composite membranes resisted fouling as shown by no drop in flux during in-plant trials and absence of foulants by IR-IRS. In contrast both hydrophobic polyvinylidene fluoride (PVdF) and polysulfone membranes showed rapid flux decline and were found by IR-IRS to be coated with essentially all of the pressate constituents after exposure to the mill effluent. PVdF membranes were examined in detail by IR-IRS to monitor membrane fouling as a function of exposure time in a laboratory permeation test cell and exposure to PSFP in a static contact test. Hydrated lignin sulfonates, as free acid or salts, were found to be the initially absorbed species, with cellulosic oligomers depositing later on the initial foulant layer. © 1998 Elsevier Science B.V.

Keywords: Ultrafiltration; Fouling; FT-IR, IRS; Effluent treatment

1. Introduction

Membrane systems can be engineered to successfully remove pollutants from many waste streams. Frequently, operational life is limited by non-reversible adsorption and pore-blocking processes. These fouling processes lead to flux reduction and sometimes loss of selectivity. These parameters have been extensively studied and are valuable engineering criteria for measuring fouling propensity [1] and references cited there in, [2–4]. However, they do not clarify the detailed deposition of solute(s) on the

membrane surface, especially the genesis of fouling. Extensive studies of single protein adsorption have been made [5,6] and references cited there in.

Effluent streams, from the various stages of the pulping processes used to produce paper, contain an array of suspended fibers and lignins, resin micelles, lignin solubles, sugars and other soluble carbohydrates and residual pulping chemicals. For this complex mixture of dissolved, colloidal and suspended materials, spectroscopic techniques can potentially augment flux information by giving more precise information on the adsorption of species on membrane surfaces. Spectroscopic techniques have been extensively used to study membrane fouling, including protein fouling [7–11]. Foulants limiting the nano-

---

*Corresponding author.

[1]Issued as NRC #41964.

and ultrafiltration of pulp mill effluents have not been well characterized other than by flux decline measurements [4,12,13].

In this paper, we explore the use of internal reflection spectroscopy (IRS), on a Fourier Transform Infrared (FTIR) spectrometer to examine the active surface of nano- and ultrafiltration membranes as they become progressively fouled. Four candidate materials of widely differing fouling propensities were examined after exposure to plug screw feed pressate so as to compare surface changes with measured changes in mill or laboratory test cell performance.

2. Experimental

2.1. Effluent Stream

In semi-chemical mechanical pulping, wood chips are chemically digested at 130°C in sulfite solution. The digested pulp is pressed to produce a heavily contaminated sulfonated liquor from the press. This aqueous liquor is used in the pre-wash of the wood chips which are then pressed to produce the plug screw feeder pressate (PSFP) (Fig. 1). A typical PSFP composition is shown in Table 1, although quite wide variations occur in practice.

2.2. Membrane types studied

The four membranes studied included two hydrophillic materials (a regenerated cellulose, YM-30, Amicon, and a polysulfone thin-film-composite, DES-5, Desalination Systems) and two hydrophobic membranes (polyvinylidene fluoride, PVdF, HFM-180 Koch Membrane Systems and polysulfone, PCI PS20 Patterson Candy International). Membrane types, molecular weight cut offs, surface compositions
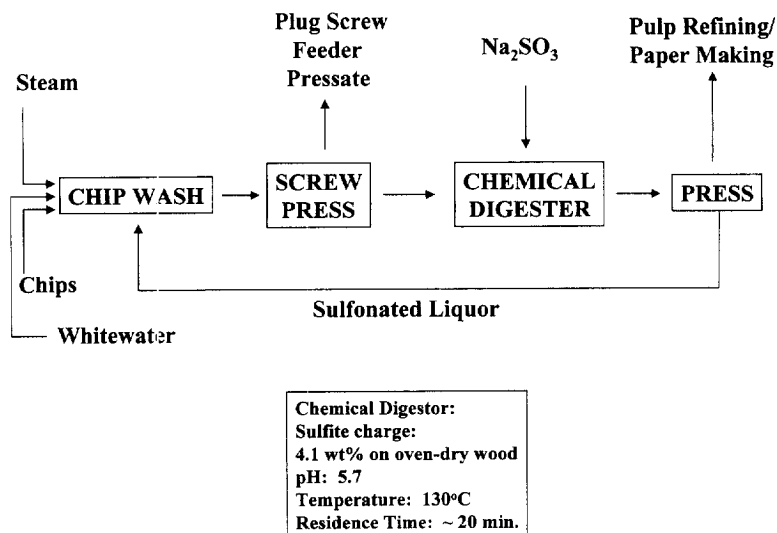
Fig. 1. Pulping Process: generation of the plug screw feeder pressate effluent (PSFP).

Table 1
Typical PSFP composition [a]

pH	Suspend solids	Dissolved solids			
		Total	Resin fatty acids	Lignin solubles	Sugars [b]
	(mg/l)	(mg l^{-1})	(mg l^{-1})	(mg l^{-1})	(mg l^{-1})
5.7	1700	12600	432	2400	2680

[a] After screening with a 100 mesh sieve.
[b] Total water soluble carbohydrates (sugars, oligomers, etc.).

Table 2
Membrane identification and performance with PSFP

Identifier	Membrane core	Surface	M. Wt. cut off (daltons) [a]	PWP [b]		Effluent flux [c]	
				Initial [d]	Final [f]	Initial [e]	Final [f]
HFM-180	Polyvinylidene fluoride (PVdF)	PVdF	>100 000	1000	141	47	16
PCI PS20	Polysulfone (PS) (Udel)	PS	>100 000	950	41	47	16
DES-5	Polysulfone (Udel)	Polyamide	200–600	14–21	25	16–33	16–33
YM-30	Regenerated cellulose	Regenerated cellulose	30 000	473–505	429	93–174	150–280

[a] Using dilute polyethylene glycol standards.
[b] Pure water permeation (l m^{-2} h^{-1}) at 345 kPa.
[c] Using PSFP under mill conditions. Flow data (l m^{-2} h^{-1}) corrected to 25°C, 345 kPa.
[d] After <1 h operation.
[e] On virgin membrane.
[f] After 4×8 h shifts of operation, spread over 4 days.

and flux/separation data are listed in Table 2, based on the methods described previously [3].

2.3. Mill-site and laboratory membrane test cells

Candidate membrane materials were exposed as 4.5 cm diameter discs to PSFP in thin channel test cells designed to give a uniform velocity profile across the radius of each disc. The test cell has been described previously [3]. In mill-site tests and in off-line, laboratory tests, membrane modules processed PSFP effluent at 50°C and 50 psi. Each membrane sample was rinsed in reverse osmosis water after testing, vacuum dried for 24 h and its active surface examined by IR-IRS.

2.4. Static contact adsorption

A series of PVdF membranes were dipped into PSFP effluent for increasing times and, after rinsing and vacuum drying, each active surface examined by IR-IRS for comparison with the samples from the mill and laboratory permeation experiments.

2.5. Membrane surface characterization

Surface composition of each as-supplied commercial membrane and of the membranes after various exposures to PSFP was examined by IR-IRS (also known as attenuated total reflection IR). The technique has been extensively applied to characterization of the membrane surfaces ([7–10,14,15]). IRS theory is also discussed in these articles and their cited refer-

ences. Briefly, IR-IRS involves placing a sample in intimate optical contact with a flat, high refractive index, IR-transmissive plate. An IR beam propagating in the plate and striking the plate-sample interface at an angle of incidence greater than the critical angle is totally internally reflected. However, at each reflection, this beam interacts with a small, but real, surface layer of the sample. A single reflection produces only a weak IR spectrum because of the small penetration into the sample but can be amplified by using the thin, flat plate as a light pipe, forcing the IR beam to undergo repeated reflections at the sample-plate interface (Fig. 2).

In our experiments, the active surface of each membrane was placed in intimate optical contact with a 50×20×2 mm^3 germanium (Ge) reflection element. Reproducible contact was achieved by the use of similar sample areas and the use of identical membrane-to-plate force, achieved by pressure plates tightened by a torque wrench as described previously (Fig. 2) [16]. The Ge element had 45° entrance and exit facets which allowed the transmitted IR beam to undergo 25 reflections before exiting to the IR detector of the Nicolet 20SX spectrometer (DTGS detector). Because of frequent contamination of the surface of the reflection element by contact with the surfaces of the fouled membranes, elements were cleaned sequentially by aqueous detergent, ethanol and vacuum drying before recording each new surface spectrum. Surface spectra were ratioed to the stored spectrum of the bare, clean Ge reflection element.

Each membrane was used only once for each permeation or contacting experiment and then rinsed in
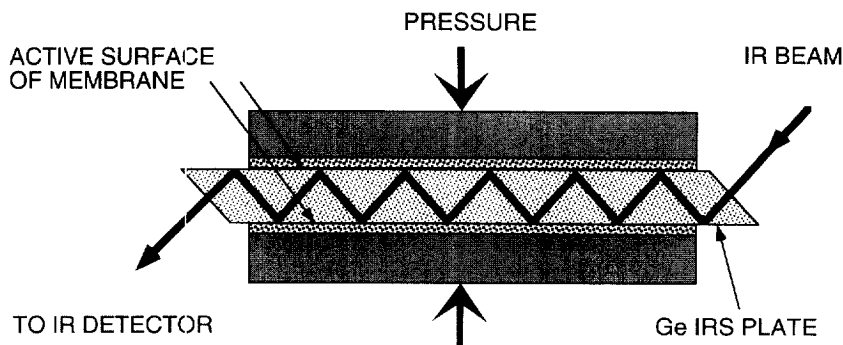
Fig. 2. IR-IRS assembly and IR reflections (cross-section, not to scale).

pure water before vacuum drying (24 h at room temperature) and then recording its IR-IRS spectrum.

IRS spectra are well known to be identical to bulk (transmission IR) spectra of the same material as far as peak location is concerned. Because the totally internally reflected beam penetrates to increasing depths of the sample with increasing wavelength, IRS spectral interactions are proportionally accentuated at longer wavelengths (lower wavenumbers). For our optical conditions (Ge at 45°C), effective depth of IR penetration ranges from 0.2 μm (at 3000 cm^{-1}) to 0.6 μm (at 1000 cm^{-1}). The reported IR-IRS spectra are not corrected for this resultant progressive increase in absorbence.

2.6. Standard materials and derivatization

Cellobiose (Sigma-Aldrich) and dehydroabietic acid (DHA, Pfaltz and Bauer) were used as a representative sugar (a cellulose oligomer) and a resin acid, respectively. The sodium salt of a sulfonated lignin (Witco) was used as a representative, water-soluble lignin. All three could be easily deposited from aqueous solution and vacuum drying on the Ge IRS plate to allow spectra to be generated for comparison with the IR-IRS spectra of the whole PSFP and foulant layer. Resin acids, soluble cellulosics and soluble, sulfonated lignins comprise a wide range of structures in each case. However, all resin acids contain carboxylic [–C(=O)–OH] or carboxylate [–C(=O)–O$^{\ominus}$] groups absorbing at about 1700 and 1550 cm^{-1}, respectively: all carbohydrates absorb at about 3400 cm^{-1} (–C–OH) and at about 1060 cm^{-1} (–C–OH or C–O–C); all sulfonic acids and sulfonates

[–S–(=O)$_2$–OH or –S–(=O)$_2$–O$^{\ominus}$] absorb at about 1180 cm^{-1}.

Because resin acids and their salts are frequent contaminants of paper-making equipment, DHA was used to establish detectability limits by IR-IRS. PVdF membranes were dipped into DHA aqueous alcohol (10% ethanol) solutions, rinsed and dried as described previously [11]. To improve the detection limits for resin acids and their salts, sulfur tetrafluoride derivatization reactions were performed on DHA-treated and mill exposed membranes, as described previously [17]. This procedure quantitatively converts the carboxylic and carboxylate groups to acid fluorides [–C(=O)F]. These have sharp IR absorptions at 1810–1850 cm^{-1}, well clear of the general PSFP IR absorptions.

3. Results

3.1. Membrane characterization by IR-IRS

Surface IR-IRS spectra of untreated YM-30, HFM-180 and PCI PS20 membranes (Fig. 3, (a, c, d)) were very similar to the IR-IRS spectra of authentic films of cellulose, polyvinylidene fluoride and poly(oxy-1,4-phenylene sulfonyl-1,4-phenylene-oxy-1,4-phenylene-isopropylidene-1,4-phenylene) (Udel) (not shown). Peak locations in all cases matched those of the well known transmission IR spectra of these polymers.

The surface of DES-5 was more complex (Fig. 3 (b)), as expected for a thin-film-composite [18]. Although dominant peaks from Udel are clearly visible (Fig. 3, (b) and (d)), after subtraction of a pure
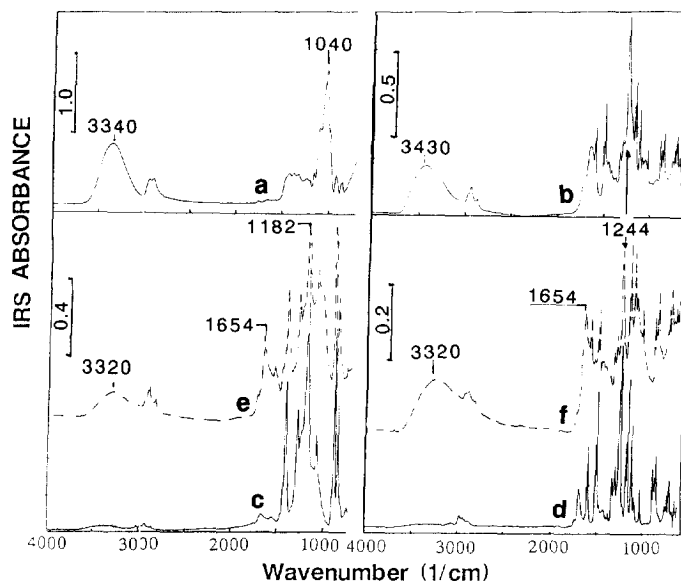
Fig. 3. IRS-IR spectra of active surfaces of membranes. (a) YM-30 (cellulose); (b) DES-5 (thin film composite on polysulfone); (c) HFM-180 (PVdF); (d) polysulfone (Udel); (e) PVdF fouled with PSFP from mill exposure; and (f) polysulfone fouled with PSFP from mill exposure.

Udel IRS spectrum (not shown), residual IR absorptions at 3400, 1630 and 1216 cm^{-1} indicated a thin (< 0.5 μm) coating (or coatings) on the Udel base. This is largely consistent with Petersen's suggestion that the top layer is a polyamide on a sulfonated Udel intermediate layer [18].

3.2. Mill-fouled membranes

Both the thin-film-composite (DES-5) and regenerated cellulose (YM-30) membranes performed well in the mill tests as shown by little or no decline in permeate flux over a total of 32 h. In contrast both the polysulfone (Udel) and polyvinylidene fluoride membranes showed a large decline in flux, consistent with extensive fouling (Table 2).

IR-IRS spectra of fouled polysulfone and PVdF surfaces are shown in Fig. 3 ((e) and (f)) after mill exposure to PSFP. Surface contamination from the PSFP is shown more clearly in Fig. 4 after spectral subtraction of the respective virgin membrane surface (that are shown in Fig. 3, (a)–(d)) from each mill-exposed membrane. As expected from the flux decline data (Table 2), YM-30 and DES-5 showed no signs of contamination (spectra largely featureless, within the limits of spectral subtraction), whereas HFM-180 and

Udel showed spectra consistent with a heavy, identical contamination. For comparison, IRS spectra of the dried PSFP and three of its expected, major ingredients (a resin acid, a soluble lignin and a sugar oligomer) are collected in Fig. 5. Because the contact area and contact quality were not controlled for these comparison spectra, absolute absorbance values are misleading and are not shown. An IRS subtract spectrum from a fouled membrane (Fig. 4 (d)) is repeated in Fig. 5 (a), for ease of comparison with the dried PSFP spectrum. The spectra of the foulant layers on HFM-180 and on Udel (Fig. 4 (c) and (d)) are similar to that of the total PSFP (Fig. 5 (a)), although the (unidentified) peak at 1654 cm^{-1} is more accentuated in the fouled surfaces than in the PSFP spectrum.

3.3. Resin acid detection

Resin acids are well recognized contaminants in paper making processes, depositing on Foudrinier wires and in other process stages and a suggested source of membrane fouling [13]. The carboxylic acid [–C(=O)–OH] and carboxylate ion [–C(=O)–O$^{\ominus}$] functional groups of resin acids and anions give rise to IR absorption at 1710–1690 cm^{-1} and 1550 cm^{-1},
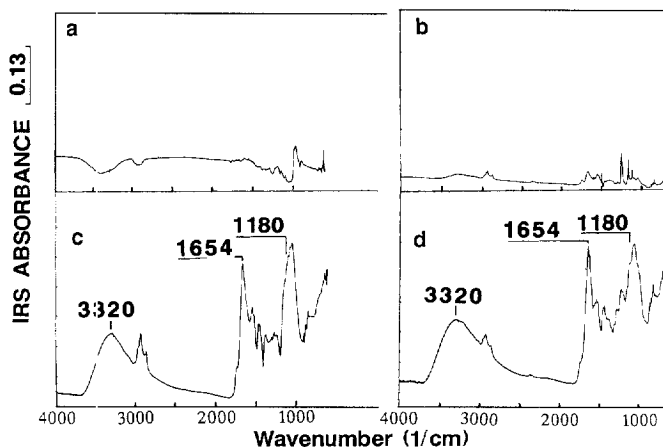
Fig. 4. IRS-IR spectra of foulants on membranes. Spectra obtained by subtraction of the spectrum of the virgin membrane from that of the mill-effluent exposed membrane. Membranes a–d as in Fig. 3.
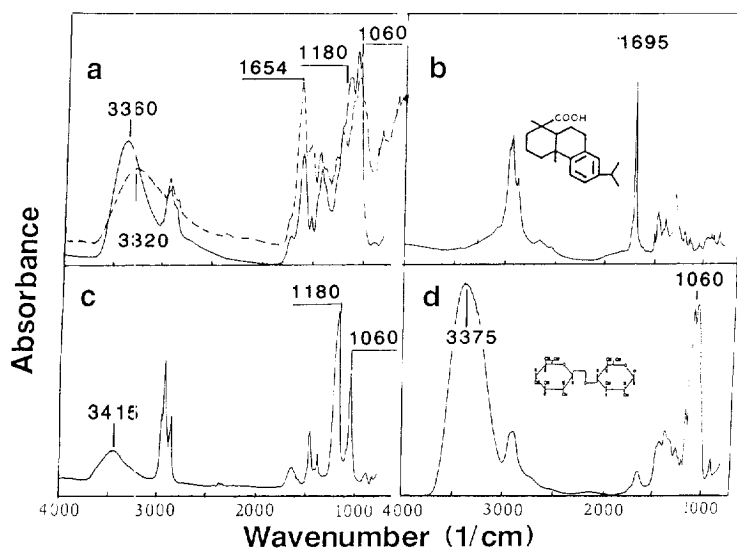

Fig. 5. IRS-IR spectra of PSFP effluent components. Samples deposited from "solution" directly onto the Ge element: (a) dried, whole PSFP mixture (– – –), surface deposit from mill exposure [(polysulfone+PSFP) – (polysulfone)] (————); (b) dehydroabietic acid; (c) lignin sulfonate, sodium salt; and (d) cellobiose.

respectively. Both absorptions would be heavily over-lapped with the total PSFP spectrum (Fig. 5 (a)) so that IR-IRS detection of resin acids is very difficult. The SF$_4$ derivatization reaction was used to enhance detectability.

To confirm the effectiveness of this derivatization process, dehydroabietic acid (DHA) was used as a model resin acid. From Fig. 6, DHA was easily

detected on PVdF with a good signal-to-noise ratio after the membrane was dipped into a 1000 ppm aqueous alcohol solution of DHA. SF$_4$ treatment replaced the 1695 cm^{-1} acid absorption with the acid fluoride band at 1825 cm^{-1}. When the SF$_4$ treatment was used on a heavily fouled PVdF membrane from the mill permeation cells, an acid fluoride absorption at $\sim$1835 cm^{-1} was clearly visible (Fig. 6).
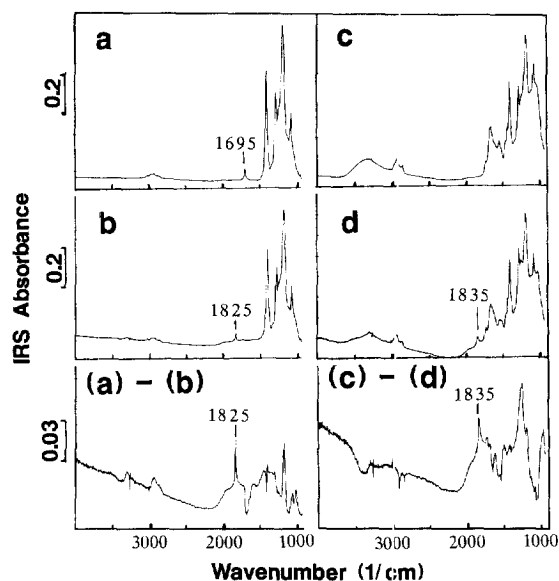
Fig. 6. IRS-IR spectra of PVdF membranes after exposure to PSFP or DHA. (a) After 24 h contact with 1000 ppm solution of DHA in 10% ethanol/water, rinsing and vacuum drying; (b) sample (a) after 24 h SF$_4$ exposure; (c) after exposure in the mill test and vacuum drying; and (d) sample (c) after 24 h SF$_4$ exposure.

3.4. Kinetics of membrane fouling

For the mill exposed membranes, at this state of extensive blockage, it is not possible to identify a dominant species or the sequence in which components of the PSFP were deposited. In an attempt to identify the critical component of PSFP which first adsorbs to initiate the fouling process, one of the readily fouled membranes was studied further under laboratory conditions. Because PVdF has the simpler IR spectrum as compared to Udel (Fig. 3 (c) and (d)), facilitating the detection of adsorbed species, a series of PVdF membranes were exposed to PSFP in the laboratory test cell. After preset time intervals of PSFP permeation, membranes were removed, rinsed in distilled water, vacuum dried and then examined by IR-IRS. Spectra of adsorbed species are shown in Fig. 7 as a function of permeation time. In these experiments, sample area and sample-to-IRS-plate contact pressure were kept constant to allow meaningful comparison of IRS spectra at increasing permeation times.

Static adsorption (dip) tests are frequently used to identify fouling by, for example, protein systems [2]. Strips of PVdF membranes were similarly dipped into
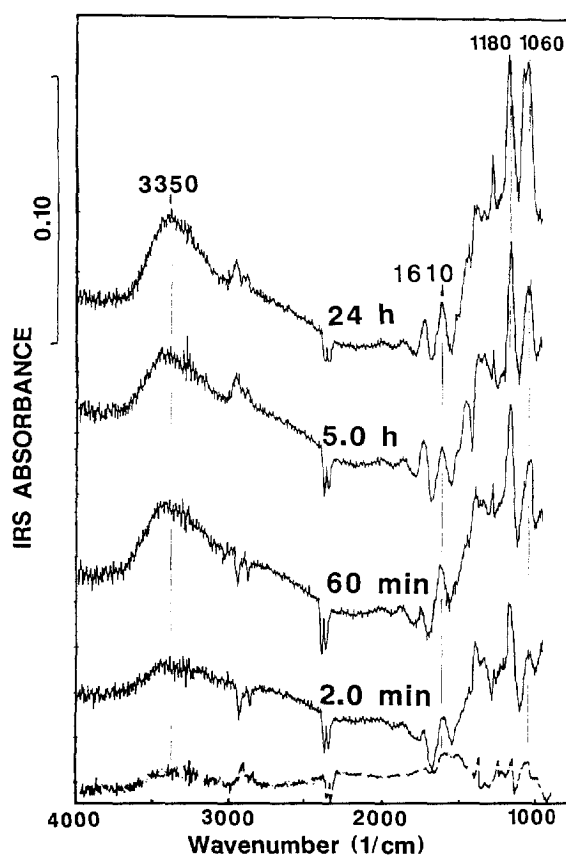

Fig. 7. IRS-IR spectra of accumulated foulant on PVdF after PSFP permeation. Spectral subtracts obtained as in Fig. 4, but membranes exposed in the laboratory permeation test cell. Times refer to duration of PSFP permeation. (– – –) (Water exposed, then dried PVdF membrane) – (virgin, as supplied, PVdF membrane).

PSFP effluent for a series of increasing times, rinsed with distilled water upon removal, vacuum dried and their active surfaces examined by IR-IRS (Fig. 8), as for the permeate exposed series.

4. Discussion

IR-IRS (or ATR-IR) has been used quite extensively to characterise the active surface of membranes, including foulant identification and pore-water interactions (7, 8, –10, 14, 15). The technique can generate IR spectra of an effective surface thickness ranging from about 0.2 to 5 μm, depending on the chosen optical conditions. While qualitative comparisons of
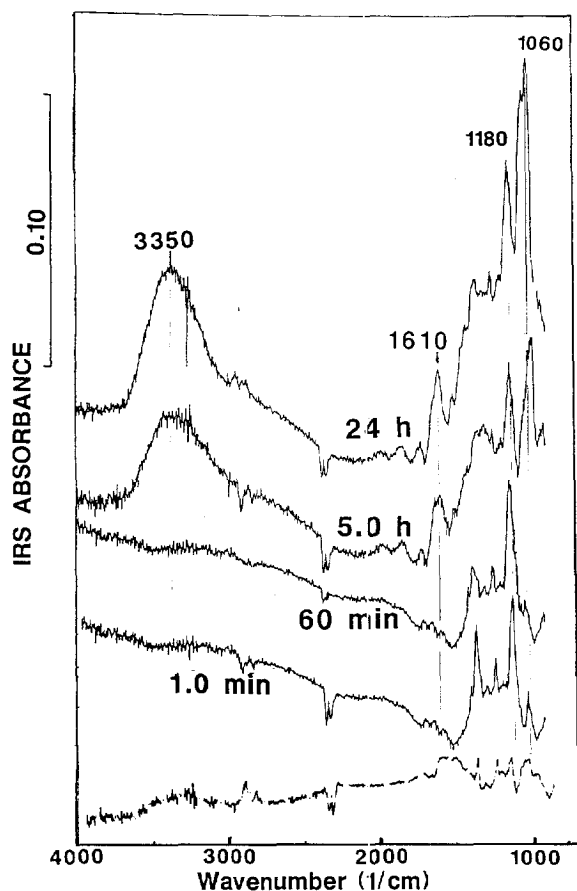
Fig. 8. IRS-IR spectra of adsorbed foulant on PVdF after dip test. Spectral subtracts obtained as in Fig. 4. Times refer to duration of membrane contact with PSFP. (– – –) (Water exposed, then dried PVdF membrane) – (virgin, as supplied, membrane).

surfaces by IR-IRS are fairly straight forward, quantitative comparisons are difficult because of the need to control the quality of optical contact. If this is not practicable (for samples of very different roughness or hardness for example), normalization to a standard IR absorption from an invariant group may allow useful quantitative intercomparison between samples.

As for transmission IR, IRS spectra show a linear dependence of absorbance on concentration. This allows the use of the FTIR's interactive spectral subtraction software, where the IRS spectrum of a (clean) reference surface is subtracted from that of a fouled surface to leave the IRS spectrum of only the foulant(s). For any one material, interactive spectral subtraction can eliminate (or suppress to be very

small) all IR peaks from the virgin material. This requires a trial and error procedure using the standard FTIR software, until a "best" subtraction (as determined visually by the operator) is reached. The residual spectrum from the subtract process then represents only surface changes, without an overlay of the spectrum of the virgin material. This extremely valuable technique can be applied successfully to IR-IRS spectra provided that spectra are of similar quality (i.e. similar numbers of reflections and similar sample-IRS plate contact). Often slight shifts in peak location result from specific interactions, making perfect subtraction impossible, as shown by some small, residual peaks of the virgin material.

From a comparison of the subtract spectra shown in Fig. 4 with the raw (unprocessed) spectra of the virgin PVdF and polysulfone membranes (Fig. 3 (c) and (d)) and the mill-fouled surfaces of these membranes (Fig. 3 (e) and (f)), subtraction is quite successful for these heavily fouled surfaces. Subtraction at low degrees of fouling (Figs. 7 and 8) is much more demanding. Because water exposure can lead to restructuring or specific pore interactions, control subtraction spectra were generated from the spectra of PVdF films exposed to water for up to 96 h. (followed by vacuum drying as usual) by subtracting the virgin (as supplied) PVdF IR-IRS spectrum. All gave quite similar subtract spectra. One example is repeated in Figs. 7 and 8, indicating negligible effect on the quality of the subtract spectra. This implies that the changes shown in Figs. 7 and 8 are real. (The doublet at 2363 and 2334 cm^{-1} is from small variations in residual carbon dioxide in the FTIR spectrometer).

IR-IRS spectra with a Ge reflection element as used in our work result from a surface layer of each membrane equivalent to about 0.2–0.6 μm thickness when a 45° angle of incidence is used [16]. Previously reported IR-IRS studies of fouled membranes have used optics leading to about 1.4 to 4.5 μm, obtained with KRS-5 elements [7,8]. Even at the low penetration obtained with Ge, in spectra of our heavily fouled PVdF and polysulfone membranes from the mill exposure, the PVdF and polysulfone peaks are still visible, over layered on the PSFP spectrum (Fig. 3 (e) and (f)). In addition, it must be remembered that IRS-spectra are integrated averages of the 5.0×10 cm^2 membrane areas examined and foulant penetration

into the pore structure cannot be differentiated from a general uniform adsorption.

From the IR-IRS spectrum of the dried PSFP (Fig. 5 (a)), PSFP is confirmed to be predominantly a mixture of soluble lignin species, such as lignin sulfonate and its salts and sugar and/or cellulosic oligomers (Fig. 5 (c) and (d)), as expected from the PSFP composition (Table 1).

From the IR-IRS subtract spectra of both the permeation and static adsorption tested PVdF membranes (Figs. 7 and 8), an initial absorption at $1180\,cm^{-1}$ is clearly visible even after 2 min or less together with a weaker $3350\,cm^{-1}$ absorption. After about 1 h in the permeation cell or about 5 h. of static adsorption, strong absorptions at 1060 and $3350\,cm^{-1}$ are also evident and continue to grow with increasing PSFP exposure times. From the spectra of the PSFP constituents (Fig. 5), the $\sim1180\,cm^{-1}$ absorption is consistent with lignin sulfonate salts or free acids preferentially adsorbing on the PVdF. Lignin sulfonate salts [as $\sim S(=O)_2-O^{\ominus}M^{\oplus}$] and hydrated free acids [as $\sim S(=O)_2-O^{\ominus}H_3O^{\ominus}$] both have a strong absorption at $1170-1190\,cm^{-1}$ and a lower intensity absorption at $1140-1160\,cm^{-1}$ from the $-S(=O)_2-O^{\ominus}$ group [19]. Associated water is detected in the IR at $\sim3350\,cm^{-1}$ (strong and very broad) and $\sim1630\,cm^{-1}$ (weak) [14]. Sulfite and bisulfite salts from the pulping chemicals (Fig. 1) would both give rise to strong $980\,cm^{-1}$ absorptions but are not detected in the PSFP (Fig. 5 (a)). The strong 3350 (–C–OH) and 1060 (–C–OH and –C–O–C–) peaks are consistent with the later adsorption of cellulosic species on top of the lignin sulfonates. The kinetics of growth of the 1180 and $1060\,cm^{-1}$ absorptions are shown in Figs. 9 and 10 for membranes from the permeation cell and static adsorption tests, respectively.

From Figs. 9 and 10, lignin sulfonate species adsorb almost immediately onto the PVdF surface. This rapid adsorption appears to correspond with the fast sorption step discussed by Belfort et al. [6]. The later detection of cellulosic material in the foulant layer is consistent with multi layer formation [6]. Large quantities of cellulosic species then progressively accumulate on this modified surface, eventually leading to severe flux reduction. For the fouling resistant membranes (the regenerated cellulose YM-30 and the thin film composite, DESAL-5 with a highly polar, hydrophillic surface), permanent adsorption of lignin sulfonate
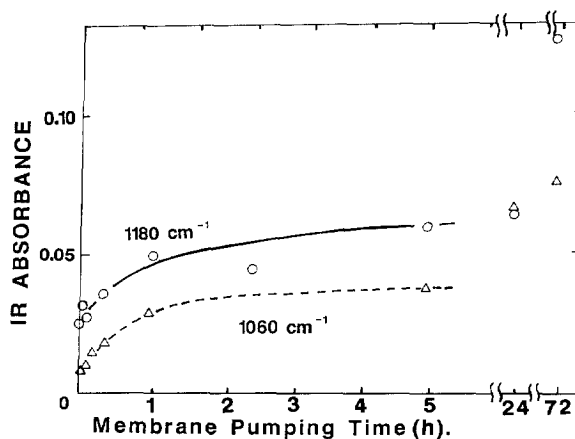

Fig. 9. Kinetics of accumulation on PVdF membranes of key foulant components from PSFP permeation. Essentially zero flux at >70 h of operation.
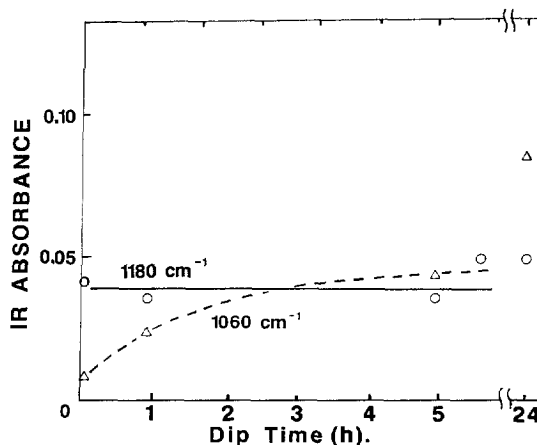

Fig. 10. Kinetics of accumulation on PVdF membranes of key foulant components from PSFP dip testing.

species is obviously unfavourable. Possibly this could be explained in terms of the dehydration of the water-solvated lignin sulfonate species on the surfaces of the more hydrophobic membranes (PVdF and polysulfone). As proposed by Ko et al. for protein-fouled UF membranes, deposition and dehydration of the lignin sulfonates on the membrane surface could lead to the progressive formation of an insoluble compact layer [2]. For the hydrophillic surfaces, water transport on these surfaces could maintain hydration of the lignin sulfonate species, preventing their permanent deposition.

During the treatment of pulp and paper effluents, constituents of "tall oil" such as resin (or rosin) acids have been suggested as gel promoters which lead to membrane fouling [13]. The IR-IRS detection limit for adsorbed resin acid such as DHA is expected to be at the 100–200 ppm level, based on peak size and signal-to-noise ratio (Fig. 6), when the SF_4 derivatization is used. IR-IRS analysis of the mill-fouled PVdF membranes after prolonged exposure to PSFP indicated the presence of only traces of carboxylic acids (Fig. 6 (d)). The observed acid fluoride band ($\sim$1835 cm^{-1}) was also more consistent with a fatty acid such as stearic acid rather than a resin acid such as DHA (at 1825 cm^{-1}) [17]. No indications of carboxylic acids were found in the early stages of dynamic or static fouling in the laboratory (0–6 h, SF_4 treated spectra not shown). Woerner and McCarthy used ether extraction to remove "tall oils" from a Kraft black liquor and showed by the negligible change in membrane flux that tall oil constituents did not contribute to membrane fouling by this pulping effluent [12].

Ramamurthy et al. have identified calcium, aluminum and silica in PSFP-fouled membranes by energy dispersive spectroscopy [13]. This technique can only detect elements with atomic number above about 11, so that the bulk of the gel layer could not be analyzed.

5. Conclusion

IR-IRS can be used in conjunction with flux decline measurements to give some information on the mechanism of membrane fouling from a complex, pulp and paper effluent stream. From a study of membrane surfaces exposed to increasing times to PSFP, surface IR spectra confirm that hydrophillic membranes are not fouled, whereas hydrophobic membranes have a much higher fouling propensity. For the readily fouled, hydrophobic membranes, IR-IRS spectra are consistent with the initial adsorption of lignin sulfonates, as free acids or salts, followed by a later deposition of cellulosic oligomers. The lower fouling propensity of highly hydrophillic membranes, implies that loss of water of hydration on the more hydrophobic membrane surfaces is the precursor to irreversible precipitation of the lignin sulfonates. Lignin sulfonates may then be useful as model foulants in

evaluating various membrane modifications for pulp and paper applications.

References

[1] G. Belfort, J.M. Pimbley, A. Greiner, K.Y. Chung, Diagnosis of membrane fouling using a rotating annular filter. Part I. Cell culture media, J. Membr. Sci. 77 (1993) 1–22.

[2] M.-K. Ko, J.J. Pellegrino, R. Nassimbene, P. Marko, Characterization of the adsorption-fouling layer using globular proteins on ultrafiltration membranes, J. Membr. Sci. 76 (1993) 101–120.

[3] M.M. Dal-Cin, C.N. Striez, T.A. Tweddle, F. McLellan, P. Ramamurthy, Membrane performance with plug screw feeder pressate: operating conditions and membrane properties, Desalination 105 (1996) 229–244.

[4] D.L. Woerner, J.L. McCarthy, Ultrafiltration of pulp mill liquors, Tappi J. 70(3) (1987) 126–130.

[5] A.D. Marshall, P.A. Munro, G. Tragardh, The effect of protein fouling in microfiltration and ultrafiltration on permeate flux, protein retention and selectivity: A literature review, Desalination 91 (1993) 65–108.

[6] G. Belfort, R.H. Davis, A.L. Zydney, The behaviour of suspensions and macromolecular solutions in crossflow microfiltration, J. Membr. Sci. 96 (1994) 1–58.

[7] M. Fontyn, K. van't Riet, B.H. Bijsterbosch, Surface spectroscopic studies of pristine and fouled membranes. Part I. Method development and pristine membrane characterization, Colloids and Surfaces 54 (1991) 331–347.

[8] M. Fontyn, K. van't Riet, B.H. Bijsterbosch, Surface spectroscopic studies of pristine and fouled membranes. Part II. Method development and adsorption mechanism, Colloids and Surfaces 54 (1991) 349–362.

[9] M. Oldani, G. Schock, Characterization of ultrafiltration membranes by infrared spectroscopy, ESCA, and contact angle measurements, J. Membr. Sci. 43 (1989) 243–258.

[10] J.D. Isner, R.C. Williams in: Analytical techniques for identifying reverse osmosis foulants, A. Amjad (Ed.), Reverse Osmosis, Van Nostrand, New York, NY, 1993, pp. 237–274.

[11] P. Spevack, Y. Deslandes, ToF-SIMS analysis of adsorbate/membrane interactions. Part I. Adsorption of dehydroabietic acid on poly(vinylidene fluoride), Appl. Surface Sci. 99 (1996) 41–50.

[12] D.L. Woerner, J.L. McCarthy, Ultrafiltration of Kraft Black Liquor, A.I.Ch.E. Symp. Ser. 232: Application of Chemical Engineering in the Forest Products Industry, 80, 1984, 25–33.

[13] P. Ramamurthy, R. Poole, J.G. Dorica, Fouling of Ultrafiltration membranes during treatment of CTMP Screw Press Filtrates, J. Pulp Paper Sci. 21(2) (1995) J50–J54.

[14] D. Murphy, M.N. de Pinho, An ATR-FTIR study of water in cellulose acetate membranes prepared by phase inversion, J. Membr. Sci. 106 (1995) 245–257.

[15] S. Hajatdoost, J. Yarwood, ATR-FTIR spectroscopic studies of the structure and permeability of sulfonated poly(ether sulfone) membranes, J. Chem. Soc., Faraday Trans. 93(8) (1997) 1613–1620.

[16] D.J. Carlsson, D.M. Wiles, Surface studies by attenuated total reflection spectroscopy. Part I. Corona treatment of polypropylene, Can. J. Chem. 48 (1970) 2397–2406.

[17] D.J. Carlsson, R. Brousseau, C. Zhang, D.M. Wiles, Identification of products from polyolefin oxidation by derivatization reactions, Amer. Chem. Soc. Symp. Ser. 364 (1988) 376–389.

[18] R.J. Petersen, Composite reverse osmosis and nano filtration membranes, J. Membr. Sci. 83 (1993) 81–150.

[19] L.J. Bellamy, Advances in Infrared Group Frequencies, Methuen, London, 1968, p. 224.